Experimental Study on the Friction Drag Reduction of Superhydrophobic Surfaces in Closed Channel Flow

M. Monfared[1†], M. A. Alidoostan[2] and B. Saranjam [1]

[1] *Mechanical Engineering, Malek-Ashtar University of Technology, Shiraz, 7194915685, Iran*
[2] *Chemical Engineering, Malek-Ashtar University of Technology, Shiraz, 7194915685, Iran*

†*Corresponding Author Email: mmonfared@mut.ac.ir*

ABSTRACT

Due to the importance of copper and its alloys in marine applications, the main objective of this research is to provide a simple, effective and low cost manufacturing approach to fabricate a superhydrophobic riblet copper surface with high drag reduction capability in laminar and turbulent flow regimes. Therefore, the riblets are produced by wire cut technique on the copper substrate and then by using a wet chemical method, a superhydrophobic coating is produced on the riblet surface. A pressure drop measurement system consists; pump, closed channel flow with a fabricated surfaces on the lower wall, connections and pressure drop transmitter is employed to measure the pressure drop in the close channel flow, for Reynolds number from 300 to 2769, in order to evaluate the ability of the fabricated surface to reduce the friction drag. The experimental results revealed that combining the abilities of the riblet and superhydrophobic surfaces increases the surface's ability to reduce friction drag. In addition, the riblet surface and superhydrophobic riblet surface on average decreased the friction drag by 10.33% and 42.65% correspondingly in water flow ranging from laminar to turbulent flow regime. Finally, according to the experimental results, the drag reduction performance of riblet surface is improved from 18.9% to 56.9% after superhydrophobic coating.

NOMENCLATURE

A	area	P	pressure
c	cavity	r	rib
D	diameter	s	width
DR	drag reduction	V	velocity
F	friction drag		
f	friction coefficient	λ	slip length
h	height	τ	shear stress
H	hydraulic	μ	viscosity
L	length	ρ	density
lam	laminar flow	θ	contact angle

1. INTRODUCTION

Friction drag at fluid-solid interface is due to shear stress on the surface and has a great importance for devices which are involved to the fluid flow. Developments of drag reduction techniques for wide range of flow regimes have large effects on the new technologies. Some benefits of drag reduction are reducing the pressure drop in pipeline systems for fluid transfer, decreasing the fuel consumption and increasing the speed of marine devices such as ships and vessels. The former drag reduction techniques include the addition of polymers, surfactants, injected air layers, wall compliance and permeability.

Philip (1972) studied the laminar viscous flow in a two-dimensional channel with ribs and cavities. The ribs and cavities were parallel to the flow. The results revealed that the slip length increased by increasing the cavity fraction. Bechert and Bartenwerfer (1989) and Choi (1989) reported that the riblets reduce drag by preventing the lateral flow in viscous sublayer. Choi *et al* (1993) by Direct Numerical Simulation represented that the drag reduction over riblets are induced by

depression of velocity and vorticity fluctuations. Bechert *et al* (1997) and Itoh *et al* (2006) showed that the highest drag reduction of riblets in turbulent channel flow is around 7%–9%. Watanabe *et al.* (1999) examined the flow through a hydrophobic circular tube and obtained 14% drag reduction. Davies *et al* (2006) considered a laminar flow channel with superhydrophobic surfaces. They indicated that the drag reduction decreased by increasing Reynolds number. Yeo *et al* (2010) designed and fabricated hydrophobic surfaces with various micropillar arrays and investigated the effect of the aspect ratio of the micropillar on the wettability of the surfaces. They found that, the micropillars with high aspect ratio enhance the hydrophobicity of the surface by increasing the surface roughness.

The shark skin-inspired riblets in closed channel flow experimentally examined by Bixler and Bushan (2013). They reported that, in turbulent water flow, the coated riblet provided the maximum pressure drop reduction of 34%, while, in turbulent air flow, the sawtooth riblet represented the maximum pressure drop reduction of 26%. Zhao and *et al* (2014) suggested a new hydrophobic model which is consistent with the special structure of shark skin inspired micro-riblets. The results showed that the surface of micro-riblets possesses obvious hydrophobicity, and the actual contact angles of different droplets residing on the riblets decrease with the increase in the droplet volume. Also According to the proposed hydrophobic model and the measurement of contact angle, they found that the arrangement and structure of the shark skin inspired micro-riblets significantly affect the surface hydrophobic property.

Barbier *et al* (2014) represented a hierarchically engineered surface that was manufactured by combined two techniques of air entrapment by nanostructures and secondary vortex generation by riblet surfaces to enhance drag reduction. They produced microgrooves and nanostructures on an aluminum surface by mechanical machining and anodizing process, respectively. They archived the maximum drag reduction of 20% in turbulent flow regimes.

Luo *et al* (2015) explained the bio-inspired drag reducing mechanism and then demonstrated the main applications of these surfaces in different fluid engineering. They results demonstrated that the attack angle is not negligible for drag reduction, and released mucus in acceleration can produce the important impact on drag reduction effect and also shark skin surfaces possess many advantages compared with the simplified and straight micro-grooved surfaces. A durable metallic surfaces by superhydrophobic nanostructures coating and mirco riblet structures is fabricated by Kim *et al* (2016). The results showed a maximum drag reduction of 36% within the turbulent region. Martin and Bushan (2016) optimized the shark inspired riblet geometries for low drag applications. They studied the three different geometries and the optimal riblet geometries and dimensions were determined.

Paul *et al* (2017) carried out wind tunnel experiments on the V-shaped riblet surfaces with height and spacing between peaks of 50 to 500 micron. They modified the riblet geometry to improve the drag reduction potential of designed surfaces. Symmetric V-shaped riblets are simulated numerically by Yang and *et al* (2017) to understand the riblet effects on the turbulent boundary layer and the skin friction reduction. A series of experiments conducted by Du *et al* (2017) to investigate the maintenance of the air layer and drag reduction on hydrophobic surfaces with random micro-structures and achieved 20% drag reduction.

Rowin *et al* (2018) evaluated the performance of riblet surfaces after applying a superhydrophobic coating by planar particle image velocimetry (PIV) measurement for different riblet tip spacing. The results revealed that the drag reduction performance of riblets improved from 1.2% to 9% after coating the surface. An airfoil with riblets investigated numerically by Zhang *et al* (2018). The results demonstrated that the pressure distribution on the airfoil is slightly changed and the Reynolds stresses are greatly reduced by the riblets.

Copper and its alloys have been one of the significant materials in industry due to its high electrical and thermal conductivities and mechanical workability. It is widely used in many applications in electronic industries and communications as a conductor in electrical power lines, pipelines for domestic and industrial water utilities including seawater, heat conductors and heat exchangers and marine propellers. Increasing efficiency of the marine propellers without any significant change in their geometric structures is great of importance. Superhydrophobic riblet copper surfaces, by reducing drag and noise, increase the marine propeller performance.

Scientists have presented many techniques such as chemical etching, electrochemical deposition, laser etching, self-assembly and sol-gel to fabricate superhydrophobic copper surfaces. Up to now, no proper method to fabricate a superhydrophobic riblet copper surface has been provided. Hence, in this research, a fast, simple, low cost and multi steps approach for preparing a super hydrophobic riblet copper surface is presented to reduce drag in both laminar and turbulent flows.

A riblet-lined closed channel (rectangular duct) internal flow was examined since its effect is less understood than with open channel external flow. The riblets are produced by wire cut technique a cooper substrate and then by using wet chemical method is covered by a superhydrophobic coating. The flow channel with a single superhydrophobic riblet surface on the bottom of the channel wall is made and by using a pressure drop measurement system which includes; pump and pressure transmitter, the ability of the new manufacturing approach for friction drag reduction is examined.

2. THEORY

In the following, the fundamental concepts which

are related to riblet and superhydrophobic surfaces are explained.

2.1 Superhydrophobic Surfaces

In laminar flow without flow separation, viscosity effects dominate the resistance to the flow. For a fluid flow over a flat plate, the wall local shear stress is equal to the production of fluid viscosity μ and the normal velocity gradient du/dy. So, the total friction drag is defined as below:

$$F = \int \tau \, dA = \int \mu \frac{du}{dy} \bigg| \, dA \qquad (1)$$

Where τ_{wall} is the wall shear stress and A_{wall} is the fluid-solid contact area. This equation states that for a given fluid, the drag could be reduced by decreasing the fluid-solid contact area and by reducing the shear stress. For industrial applications, reducing the viscosity is not practical. So, the normal velocity gradient or fluid-solid contact area should be reduced. In a laminar fully developed channel flow the shear stress distribution is linear with the shear stress greatest at the walls and equal to zero at the channel centerline. When the velocity gradient at the walls is reduced the shear stress distribution remains linear but the slope of the shear stress distribution is decreased thus indicating a lower shear stress at the walls.

In turbulent flow, the viscous effects are limited in viscous sub layer. Hence, the most of transport phenomena are due to turbulent motions or unsteady eddies. The total local shear stress is:

$$\tau = \tau + \tau = \mu \frac{d\overline{u}}{dy} - \rho \overline{u'v'} \qquad (2)$$

Where $\overline{u}$, u' and v' represents the time-mean velocity and fluctuating velocity in the x and y directions, respectively.

Equation 2 states that the total local shear stress is the sum of viscous stress and turbulent stress.

superhydrophobic surfaces is one of the approaches that is applied to increase the contact area and reduce the average wall shear stress. The lotus leaf is a good example of a superhydrophobic surface which is found in the nature. The lotus leaf is a rough surface which consists of microstructures. These microstructures usually have the heights of 10-20μm and widths of 10-15μm and are coated with a waxy skin which acts as a hydrophobic coating .The combination of the microstructures and the hydrophobic coating will form a superhydrophobic surface [Daniello (2009) and Bhushan *et al* (2011)].

A schematic illustration of a superhydrophobic surface is shown in Figure 1. The air traps between microstructures and a liquid-gas meniscus form across each cavity. At the liquid-gas interface, the shear stress is very smaller than the shear stress at the liquid-solid interface. The qualitative differences between the shear stress

across a liquid-gas and liquid-solid interfaces are illustrated in Figure 2. In this figure, w_r and w_s represent the rib and cavity widths, respectively.
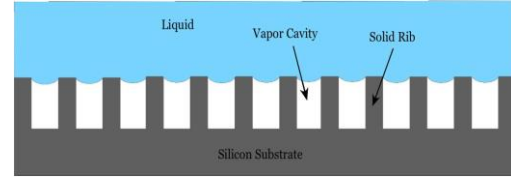

Fig. 1. Schematic illustration of a fluid flow over a superhydrophobic surface [Park *et al* (2006)].
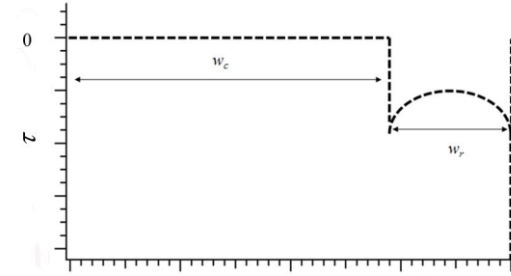

Fig. 2. Schematic illustration of Shear stress distribution across a single rib and cavity [Park *et al* (2006)].

The qualitative streamwise velocity distribution along the top of the rib and cavity for a fluid flowing above a superhydrophobic surface is illustrated in Figure 3. The figure indicates that along the rib surface the no slip condition is maintained with zero velocity. Along the liquid-gas interface the liquid velocity exhibits a finite value with a maximum at the centerline of the cavity. The integral average velocity along the rib/cavity width will be non-zero, and gives rise to an apparent macroscopic slip velocity at the surface.

The macroscopic slip velocity can also be related to a slip-length, λ, with the slip-length being defined as the wall-normal location where the fluid velocity would vanish. Navier first proposed the slip boundary condition and showed that the slip velocity, u_{slip}, was proportional to the strain rate in the fluid at the wall:

$$u = \lambda \frac{du}{dy} \qquad (3)$$

Also, one of the main parameter for investigation of a superhydrophobic surface is contact angle, θ, which characterizes the degree of wetting on a surface. Superhydrophobic surfaces exhibit contact angle greater than 150º.

2.2 Riblet Surfaces

The mechanism by which the riblets surfaces reduce the drag, is very complicated and is not yet completely obvious. As represented in Figure 4, the riblets reduce drag by preventing the cross-stream translation of the streamwise vortices in the viscous sublayer. So, by preventing the translation of vortices, the momentum transfer in the outer

boundary layer will decreased [Bechert *et al* (1997) and Dean (2011)].

At the first moment it seems that for riblet surfaces, the wetted surface is increased. So, the shear stress at the surface increases and thus the drag should increases too. But, the vortices remain above the riblets and the high-speed velocity flow does not enter in the valley. The low-speed velocity flow produces the low shear stress in the valley. Thus, the total shear stress will decreases.
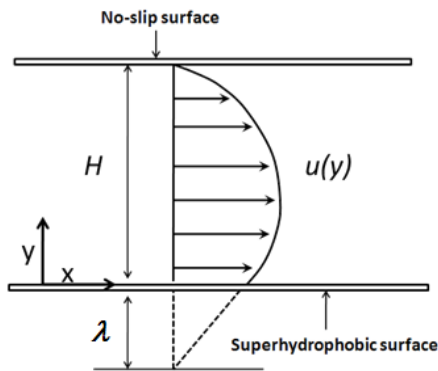

Fig. 3. Schematic illustration of Slip velocity at superhydrophobic surface [Park *et al* (2006)].
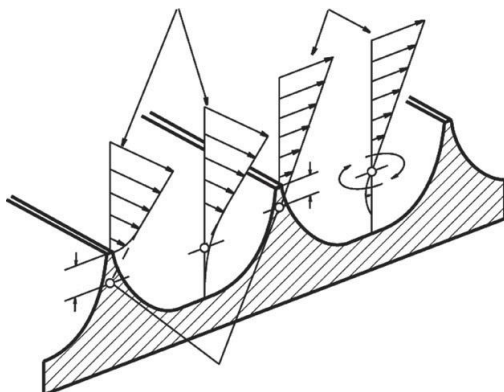

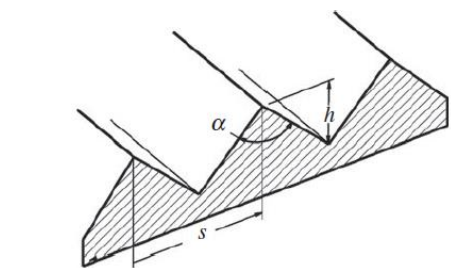**Fig. 4. Longitudinal and cross-flow on a riblet surface [Bechert *et al* (1997)].**

The riblets have cross-sectional shapes of sawtooth, scalloped and blade that are illustrated in Fig. 5. Major parameters for riblet include spacing (s), height (h) and thickness (t), which are crucial parameters to achieve the best drag reduction.

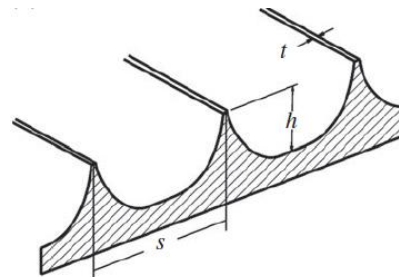## 3. FABRICATION OF A SUPERHYDROPHOBIC RIBLET SURFACE

A superhydrophobic surface by low surface energy and high contact angle has a high ability to reduce drag. Also, riblet surfaces, by preventing the cross-stream translation of vortices, reduce the total shear stress on the surface. So, by utilizing the abilities of these two types of surfaces, a surface can be achieved with high capability to reduce friction drag in laminar and turbulent flows. Furthermore, it is so

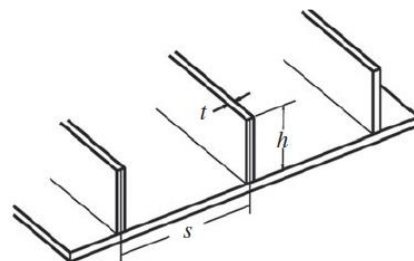important to attain a simple and low cost method to produce such a surface.

Therefore, first, a cooper substrate is used as a base plate and the wire-cut technique is employed to create the riblets on this substrate. The wire has a diameter of 150μm. Thus, the scalloped riblets with s=150±15μm and h=75±10μm is produced on the cooper substrate. Figure 6 represents the riblet surface which is fabricated by wire-cut technique. The number of riblets which are produced on the surface are about 100.

a) Sawtooth riblets

b) Scalloped riblets

c) Blade riblets

Fig. 5. Schematic illustration of different cross-sectional shapes of riblets [Bechert et al (1997)].

In the following, a wet chemical method is utilized to cover the riblets by a superhydrophobic coating. The surface is polished by silicon sandpaper with grades 400 to 1000 and is degreased by acetone. The surface is washed by distilled water and then dried. The riblet surface is immersed in the nitric acid (13%) for 15 seconds to remove the oxides on the surface. In addition, to produce the irregular roughness on the riblets, the surface is dipped in the solution of H_2O 54ml, CH_3COOH 0.02ml, HCL 37% 0.06ml, for 12 hours and then dried in N_2 fluid flow. then by immersing the surface into solution of ethanol thetradecanoic acid 0.1M at 37°c for 10 days, a superhydrophobic coating is deposited on the riblet surface and a superhydrophobic riblet

surface is fabricated (Figure 7). The camera picture of water droplet on the fabricated superhydrophobic riblet surface is represented in Figure 8. As it clear, the fabricated surface is superhydrophobic surface.
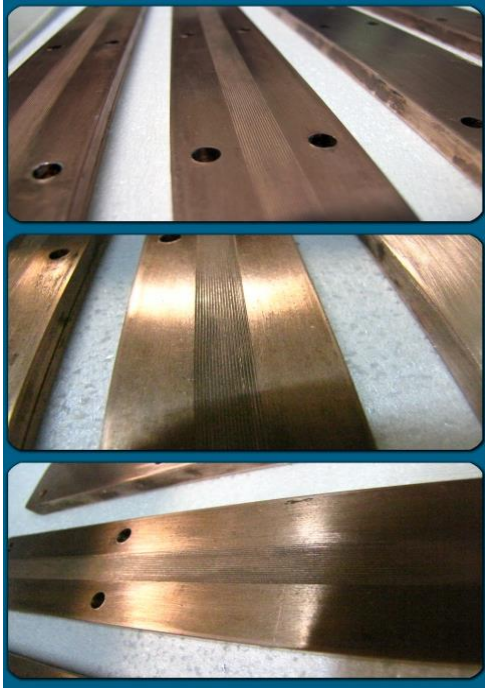

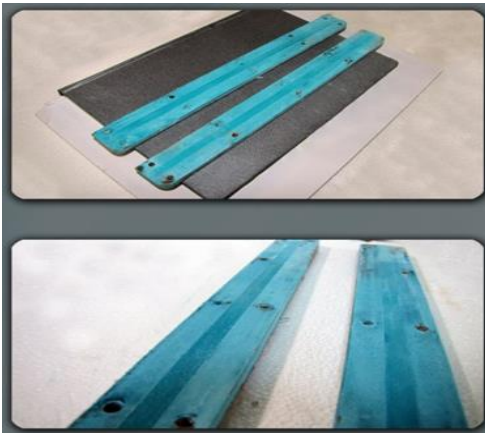**Fig. 6. Fabricated scalloped riblets surface.**

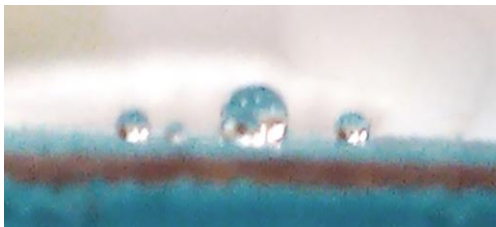**Fig. 7. Fabricated superhydrophobic riblet surface.**

Fig. 8. Camera picture of water droplet on the superhydrophobic riblet surface.

4.   EXPERIMENTAL SETUP

In this research, by using the pressure drop measurement technique which measures the pressure drop in a closed channel flow, the ability of the superhydrophobic riblet surface to reduce the pressure drop is evaluated. The fabricated surfaces is installed on the lower wall of the channel. In the closed channel flow, a pressure drop have a direct relation with friction coefficient as a below:

$$\Delta P = \frac{\rho V\ fL}{2D} \tag{4}$$

So, the drag reduction is achieved by:

$$DR(\%) = \frac{\Delta P - \Delta P}{\Delta P} \tag{5}$$

Where, ΔP_s and ΔP_{RS} are the pressure drop for the closed channel flow with simple surfaces and superhydrophobic riblet surfaces, respectively.

The experimental setup consists; pump, connections, pressure drop transmitter and closed channel flow (Figure 9). The height and width of the channel are 2mm and 7 mm, respectively (Figure 10). The bottom wall has a length of 30 cm and the pressures are measured by pressure transmitter which put in the distance of 5cm and 25 cm from the flow inlet. Additionally, the flow rate is set from 5L/h to 50L/h by a rotameter.

Fig. 9. Experimental setup for measuring pressure drop across the closed channel flow.

Fig. 10. Closed channel flow.

5.   EXPERIMENTAL RESULTS

The experiments are carried out for three different conditions. The closed channel with a single simple surface, riblet and superhydrophobic riblet surfaces on the bottom. Also to reduce the experimental

Table 1 Pressure drop across a closed channel flow

Flow rate (L/h)	Re	ΔP_S (mbar)	ΔP_{SH} (mbar)	ΔP_{SHR} (mbar)
5	307	0.65	0.63	0.26
10	615	1.43	1.32	0.58
15	923	2.10	1.83	0.87
20	1230	3.38	2.90	1.44
25	1538	4.45	3.90	2.11
30	1845	5.55	5.05	2.96
35	2153	6.92	6.13	4.15
40	2460	8.60	7.68	5.70
45	2769	10.00	8.90	7.01

Table 2 Uncertainty of the measured pressure drop across a closed channel flow

a: A closed channel flow with simple surface

Re	U_V	U_L	U_{Dp}	U_t	$U_t/ \Delta P$ (%)
307	8.60E-03	1.19E-04	4.36E-03	9.64E-03	1.48%
615	1.09E-02	1.19E-04	1.02E-02	1.49E-02	1.04%
923	1.93E-02	1.19E-04	1.45E-02	2.42E-02	1.15%
1230	2.87E-02	1.19E-04	2.16E-02	3.59E-02	1.06%
1538	2.93E-02	1.19E-04	2.80E-02	4.05E-02	0.91%
1845	4.74E-02	1.19E-04	3.77E-02	6.05E-02	1.09%
2153	5.56E-02	1.19E-04	5.19E-02	7.61E-02	1.10%
2460	1.13E-01	1.19E-04	6.62E-02	1.31E-01	1.52%
2769	9.91E-02	1.19E-04	7.90E-02	1.27E-01	1.27%

b: A closed channel flow with riblet surface

Re	U_V	U_L	U_{Dp}	U_t	$U_t/ \Delta P$ (%)
307	1.05E-02	1.19E-04	4.73E-03	1.15E-02	1.82%
615	2.78E-02	1.19E-04	1.02E-02	2.96E-02	2.24%
923	1.83E-02	1.19E-04	1.35E-02	2.27E-02	1.24%
1230	3.23E-02	1.19E-04	2.09E-02	3.85E-02	1.33%
1538	3.20E-02	1.19E-04	2.69E-02	4.18E-02	1.07%
1845	3.50E-02	1.19E-04	3.69E-02	5.08E-02	1.01%
2153	4.89E-02	1.19E-04	4.66E-02	6.75E-02	1.10%
2460	6.25E-02	1.19E-04	6.07E-02	8.71E-02	1.13%
2769	1.15E-01	1.19E-04	7.65E-02	1.38E-01	1.55%

c: A closed channel flow with superhydrophobic riblet surface

Re	U_V	U_L	U_{Dp}	U_t	$U_t/ \Delta P$ (%)
307	1.05E-02	1.19E-04	4.73E-03	1.15E-02	1.82%
615	2.78E-02	1.19E-04	1.02E-02	2.96E-02	2.24%
923	1.83E-02	1.19E-04	1.35E-02	2.27E-02	1.24%
1230	3.23E-02	1.19E-04	2.09E-02	3.85E-02	1.33%
1538	3.20E-02	1.19E-04	2.69E-02	4.18E-02	1.07%
1845	3.50E-02	1.19E-04	3.69E-02	5.08E-02	1.01%
2153	4.89E-02	1.19E-04	4.66E-02	6.75E-02	1.10%
2460	6.25E-02	1.19E-04	6.07E-02	8.71E-02	1.13%
2769	1.15E-01	1.19E-04	7.65E-02	1.38E-01	1.55%

errors, every test is done fourth times. The results for different Reynolds number and conditions are given in Table 1. Furthermore, subscripts S, SH and SHR denote to superhydrophobic and superhydrophobic riblet surfaces, correspondingly.

In addition, Uncertainty of the experimental results are presented in Table 2. The uncertainty (U) of the experimental results consists of two components of bias (B) and precision (P), the total bias and precision limits have been obtained by the root sum squared of bias errors and standard deviation of the measured values of pressure drop across the channel. Therefore, the uncertainty analysis of the experimental data is carried out based on the frequency of repeating each test as well as the

accuracy of the equipment and presented in Table 2. Moreover, subscripts of V, L, D_p and t refer to the velocity, length, pressure transmitter and total uncertainties, respectively.

Figure 11 represent the friction drag reduction with respect to the Reynolds number for riblet and superhydrophobic riblet surfaces. The results showed that, the riblet surface reduces the drag from 4% to 14% for laminar up to the turbulent flow regimes. The mean friction drag reduction is achieved about 10.33%. The riblet surface has higher performance in turbulent flow which is due to prevent the cross-stream translation of the stream wise vortices in the viscous sublayer and enter the high speed flow in the valley. In contrast, the superhydrophobic riblet surface reduces the drag from 58% to 21% for laminar up to the turbulent flow regimes. The superhydrophobic riblet surface has the higher ability in the laminar flow and by increasing Reynolds number, Re, the performance of this surface is decreased. By increasing Reynolds numbers, the effects of superhydrophobic coating on the drag reduction is decreased. The mean friction drag reduction for superhydrophobic riblet surface is obtained about 42.65%. Additionally, according to the experimental results, the drag reduction ability of riblet surface is increased from 18.9% to 56.9% after superhydrophobic coating. So, it could be conclude that the combination of the abilities of riblet surfaces and superhydrophobic surfaces increase the friction drag reduction for wide range of the flow from laminar up to turbulent flow.
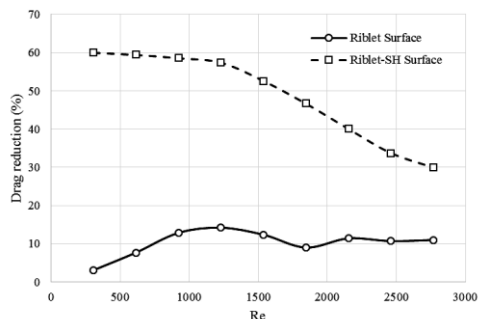

Fig. 11. Friction drag reduction versus Re. No for riblet and superhydrophobic riblet surfaces.

6. CONCLUSION

This research consists of two main parts. The main purpose of the first part is to provide a simple, efficient and inexpensive method for producing copper surfaces with high ability for drag reduction in laminar and turbulent flow regimes. The proposed method is a combined approach including a grinding method for producing regular riblet on the surface and finally a wet chemical method, which consists of several steps, to create a superhydrophobic coating on the riblet surface. Also the main goal in the second part is to establish a laboratory system to assess the ability of the fabricated surfaces to reduce the drag in laminar

and turbulent flow regimes. Therefore, an experimental setup includes; pump, channel, connections and pressure drop transmitter is designed to evaluate the ability of the superhydrophobic riblet surface for drag reduction. Experiments are performed for three different conditions: a closed channel flow with simple surface, riblet surface and superhydrophobic riblet surface. The results showed that, the riblet surface has higher efficiency in turbulent flow which is due to prevent the cross stream translation of vortices and decrease the total wall shear stress. While, the superhydrophobic riblet surface has higher ability to reduce friction drag in laminar flow. In addition, the riblet surface and superhydrophobic riblet surface on average reduced the friction drag by 10.33% and 42.65% respectively. Furthermore, the drag reduction capability of riblet surface is enhanced from 18.9% to 56.9% after superhydrophobic coating. So it could be concluded that to reduce the friction drag in a wide range of the flow from laminar up to turbulent flow regimes, the riblet and Superhydrophobic advantages should be combined Simultaneously.

REFERENCES

Barbier, C., E. Jenner and B. Durso (2014). Large drag reduction over superhydrophobic riblets. *arXiv Preprint arXiv*, 1406.0787.

Bechert, D. and M. Bartenwerfer (1989). The viscous flow on surfaces with longitudinal ribs. *Journal of Fluid Mechanics* 206, 105–129.

Bechert, D., W. Bruse, M. Hage, W. Van Der Hoeven and G. Hoppe (1997). Experiments on drag reducing surfaces and their optimization with an adjustable Geometry. *Journal of Fluid Mechanics* 338, 59-87.

Bhushan, B. and Y. Jung (2011). Natural and biomimetic artificial surfaces for superhydrophobicity, self-cleaning, low adhesion, and drag reduction. *Progress in Materials Science* 56, 1–108.

Bixler, D. and B. Bhushan (2013). Shark skin inspired low-drag microstructured surfaces in closed channel flow. *Journal of Colloid and Interface Science* 393, 384–396.

Choi, H., P. Moin and J. Kim (1993). Direct numerical simulation of turbulent flow over riblets. *Journal of Fluid Mechanics* 255, 503–39.

Choi, K. (1989). Near wall structure of a turbulent boundary layer with riblets. *Journal of Fluid Mechanics* 208, 417-458.

Daniello, R. (2009). Drag reduction in turbulent flows over micropatterned superhydrophobic surfaces. *Master of Science in Mechanical Engineering*, University of Massachusetts.

Davies, J., D. Maynes, B. Webb and W. Woolford (2006). Laminar flow in a microchannel with super-hydrophobic walls exhibiting transverse

ribs. *Phys. Fluids*. 18, 087110.

Dean, D. (2011). *The effect of shark skin inspired riblet geometries on drag in rectangular duct flow*, Doctoral Dissertation, The Ohio State University.

Dua, P., J. Wena, Z. Zhang, D. Song, Q. Hu (2017). Maintenance of air layer and drag reduction on superhydrophobic surface. *Ocean Engineering* 130, 328–335.

Itoh, M., S. Tamano, R. Iguchi, K. Yokota, N. Akino, R. Hino and S. Kubo (2006). Turbulent drag reduction by the seal fur surface. *Phys. Fluids* 18(6), 95-102.

Kim, T., R. Shin, M. Jang, J. Lee, C. Park and S. Kang (2016). Drag reduction using metallic engineered surfaces with highly ordered hierarchical topographies: nanostructures on micro-riblets. *Applied Surface Science.*

Luo, Y., Y. Yuan, J. Li and J. Wang (2015) Boundary layer drag reduction research hypotheses derived from bio-inspired surface and recent advanced applications. *Micron* 79, 59-73.

Martin, S. and B. Bhushan (2016) Modeling and optimization of shark-inspired riblet geometries for low drag applications. *Journal of Colloid and Interface Science* 474, 206-215.

Park, H. and D. Byun (2006). Drag reduction on micro-structured super-hydrophobic surface. *IEEE*.

Paul, D., S. Brian, W. Baker and P. Yagle (2017). Design and testing of conventional and 3-D riblets. *American Institute of Aeronautics and Astronautics*.

Philip, J. (1972). Flows satisfying mixed no-slip and no-shear condition. *Journal of Applied Mathematics and Physics* 23, 353–371.

Rowin, W., J. Hou and S. Ghaemi (2018). Turbulent channel flow over riblets with superhydrophobic coating. *Experimental Thermal and Fluid Science* 94, 192-204.

Watanabe, K., Y. Udagawa and H. Udagawa (1999). Drag reduction of Newtonian fluid in a circular pipe with a highly water-repellent wall. *Journal of Fluid Mechanics* 381, 225–238.

Yang. Y., M. Zhang and L. Song (2017). Numerical investigation of V-shaped riblets and an improved model of riblet effects. *Journal of Mechanical Engineering Science* 10, 1-10.

Yeo, J. and D. Kim (2010). The effect of the aspect ratio on the hydrophobicity of microstructured Polydimethylsiloxane (PDMS) robust surfaces. *Microsyst Technol* 16, 1457–1463.

Zhang, Y., H. Chen, S. Fu and W. Dong (2018). Numerical study of an airfoil with riblets installed based on large eddy simulation. *Aerospace Science and Technology* 78, 661–670

Zhao, D., Q. Tian. M. Wang and J. Jin (2014). Study on the Hydrophobic Property of Shark-Skin-Inspired Micro-Riblets. *Journal of Bionic Engineering* 11, 296–302.